Journal of Colloid and Interface Science 467 (2016) 220–229

Contents lists available at ScienceDirect

Journal of Colloid and Interface Science

journal homepage: www.elsevier.com/locate/jcis

Electrospray synthesis and properties of hierarchically structured PLGA TIPS microspheres for use as controlled release technologies

Salman A. Malik [a], Wing H. Ng [a], James Bowen [b], Justin Tang [c], Alessandro Gomez [c], Anthony J. Kenyon [a,*], Richard M. Day [d,*]

[a] Department of Electronic & Electrical Engineering, University College London, London WC1E 7JE, UK
[b] School of Chemical Engineering, University of Birmingham, Birmingham B15 2TT, UK
[c] Department of Mechanical Engineering & Materials Science, Yale University, New Haven, CT 06520-8286, USA
[d] Division of Medicine, University College London, London WC1E 6JJ, UK

GRAPHICAL ABSTRACT

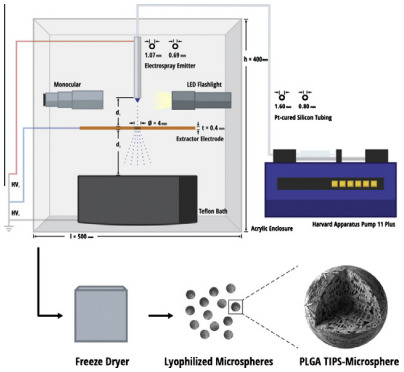

ARTICLE INFO

Article history:
Received 7 October 2015
Revised 22 December 2015
Accepted 11 January 2016
Available online 12 January 2016

Keywords:
Electrosprays
Poly(lactic-co-glycolic acid) (PLGA)
Microspheres
Thermally induced phase separation (TIPS)

ABSTRACT

Microsphere-based controlled release technologies have been utilized for the long-term delivery of proteins, peptides and antibiotics, although their synthesis poses substantial challenges owing to formulation complexities, lack of scalability, and cost. To address these shortcomings, we used the electrospray process as a reproducible, synthesis technique to manufacture highly porous (>94%) microspheres while maintaining control over particle structure and size. Here we report a successful formulation recipe used to generate spherical poly(lactic-co-glycolic) acid (PLGA) microspheres using the electrospray (ES) coupled with a novel thermally induced phase separation (TIPS) process with a tailored Liquid Nitrogen (LN_2) collection scheme.

We show how size, shape and porosity of resulting microspheres can be controlled by judiciously varying electrospray processing parameters and we demonstrate examples in which the particle size (and porosity) affect release kinetics. The effect of electrospray treatment on the particles and their physicochemical properties are characterized by scanning electron microscopy, confocal Raman microscopy, thermogravimetric analysis and mercury intrusion porosimetry. The microspheres manufactured here have successfully demonstrated long-term delivery (i.e. 1 week) of an active agent, enabling sustained release of a dye with minimal physical degradation and have verified the potential of scalable electrospray technologies for an innovative TIPS-based microsphere production protocol.

* Corresponding authors.
E-mail addresses: a.kenyon@ucl.ac.uk (A.J. Kenyon), r.m.day@ucl.ac.uk (R.M. Day).

http://dx.doi.org/10.1016/j.jcis.2016.01.021
0021-9797/

1. Introduction

The predictions by Park et al. for the 3rd generation of controlled drug delivery technologies has provided evolutionary direction to the development of engineering a novel class of release systems [1]. One of the key challenges associated with (but not fully addressed by) the previous (2nd) generation is progression towards 'modulated delivery systems'. Delivering active molecules with the desired release kinetics requires an understanding of the physicochemical properties of the delivery vehicle and its release mechanism. Establishing performance metrics using *in vitro* models is considered the 'gold standard' approach preceding clinical investigation. It is vital to recognize the complexity associated with developing new release technologies and the simultaneous influence of multiple factors. Factors such as optimized formulation, manufacturability, materials, a suitable delivery route and the *in vitro in vivo* correlation (IVIVC) to assist quality control can be considered as the benchmark prior to *in vivo* investigation.

The global market for microspheres has seen a steady growth rate in double digits in the last decade due to their use in healthcare, personal care, and in many speciality research and development applications [2]. They have been recognized as novel technologies for modulated release devices and have received significant interest from clinical communities. Polymeric microspheres are small spherical microparticles of a size ranging from 1 μm to 1000 μm that offer functionality for application-specific industries. They have a number of interesting attributes that make them particularly suitable for microencapsulation: (i) controlled release of encapsulated materials, (ii) protection of the encapsulated materials against degradative reactions which can also result in an improved shelf life and (iii) high surface-to-volume ratios [3,4].

Maintaining control of their homogeneous size, shape, skeletal porosity and reproducibility can dictate their performance in biological microenvironments. Encapsulation, biocompatibility and active agent release from microspheres are closely related to their structural properties. For example, the release rates of active molecules depend on the degradation of the polymer and/or diffusion of active molecules. This can be controlled by the molecular mass of the polymer, the microsphere size and also its porosity. The shape of a particle also influences its biocompatibility, for example, its interactions with macrophages [5–7].

Current methods for generating spherical, porous microstructures rely on techniques such as emulsion polymerization, thermal phase separation and spray drying. These techniques suffer from poor monodispersity, harsh solvent toxicities, additives and costly starting materials not scalable for pharmaceutical industries [8–11]. Achieving a high degree of control over particle structure with a scalable, continuous spray process poses a challenge and provides the primary motivation for developing and demonstrating an electrospray (ES) synthesis method for continuous particle manufacture.

This work focuses on the controlled manufacturing of polymeric microspheres using ES atomization combined with a novel thermally induced phase separation process (TIPS) followed by subsequent lyophilisation. Lyophilisation is an established robust method for the formulation of biological products, and an invaluable tool for prolonging shelf life and stability for biological drugs and vaccines. The global market for lyophilisation is projected to be worth $5.125 billion in 2019 [12], spurred by the strong growth of new drug-carriers. In this article, the formulation recipe for microsphere production is discussed with emphasis on how the role of the solution properties and ES processing parameters can determine particle shapes and sizes. Trade-offs in particle size, shape and porosity make ES aerosols a highly controllable and attractive synthesis technique, as careful engineering of poly(lactic-co-glycolic acid) PLGA microspheres has been shown to impact release kinetics and encapsulation efficiencies [13–15]. Many studies successfully report the protocols adopted to synthesize particles but fail to document a thorough physical characterization and shape analysis of the manufactured particles (i.e. size, circularity, porosity) [13,16–22]. This study addresses this need through characterization of the particles produced using ES-technology.

ES has proven to be a versatile method to manufacture particles, giving tight control over size with quasi-monodisperse size distributions. It is a liquid atomization technique that relies on electrical forces induced via electric charging of conductive media to aerosolize a liquid and generate a uniform population of highly charged, fine liquid droplets over a broad size range [23–25]. Electrostatic forces overcome the surface tension of the liquid surface causing the formation of a jet and its subsequent disintegration into droplets. The droplets obtained by this method are charged, up to a fraction of the Rayleigh limit. The charge and size of the droplets can be controlled to some extent by adjusting the liquid flow rate applied to the emitter for solution atomization and subsequently the in-flight synthesis of particles. Control over the trajectory of these particles can be precisely manipulated by the use of electric fields to drive them to/into a grounded substrate. By careful selection of a suitable solvent, operational parameters such as electric field strength can be controlled to overcome the surface tension of the liquid meniscus at the capillary tip elongating the droplet deformation into a conical shape, which snaps into a cone-like protrusion (also known as the Taylor cone), from the apex of which emission begins generating a fine jet [26]. When operated in the cone-jet mode [27,28], ES offers exquisite control of droplet size and dispersion, up to monodispersity [29]. Importantly, it does so over several orders of magnitude, from micrometer droplets to nanometer sizes, the latter being virtually impossible to generate from any other spray technique. Furthermore, the highly unipolar-charged droplets are self-dispersing in space, as a result of their mutual Coulombic repulsion, resulting in the absence of droplet coagulation [30]. By altering the solution conductivity or liquid flow rate, it is possible to control the size of the ES-particles as the diameter monotonically increases with both variables [31].

Poly(α-hydroxyesters), such as PLGA are the most common material used for the encapsulation of peptides or proteins, as they are mechanically strong, hydrophobic, biocompatible and degrade into toxicologically acceptable products that are eliminated from the body [5]. Previous studies have demonstrated the functional release of active agents from electrosprayed PLGA particles while demonstrating these highlighted properties [16,17,22]. From a clinical perspective, PLGA polymers have been widely used in marketed products [32]. Risperdal Consta has been developed by Johnson & Johnson for delivering risperidone as a commercial microsphere-based delivery system to treat schizophrenia. The excellent clinical safety record of PLGA when used as a synthetic biomaterial provides sound motivation, along with its ease of processing (using ES) to apply to our novel TIPS process; a process that has been reported in previous studies [33–35].

2. Materials and methods

2.1. Materials

Acid terminated PLGA (Purasorb PDLG 5004A, 50:50 DL-lactide/glycolide copolymer) was obtained from Corbion Purac (Netherlands). Dimethyl carbonate (DMC) (Reagent Plus 99%), Formic acid (Reagent grade ⩾95%) and Rhodamine 6G (Dye content 99%) were all purchased from Sigma–Aldrich (Poole, UK). Rhodamine 6G (R6G) was used as a drug surrogate to monitor release. Liquid

Nitrogen (LN_2) was purchased from the British Oxygen Company (BOC) (London, UK). All materials were used as received.

2.2. Synthesis of PLGA TIPS microspheres

Electrospray synthesis of polymeric particles was realized using the experimental setup sketched in Fig. 1a. A 5% (w/v) polymer solution of PLGA (Purasorb PDLG 5004A, 50:50 DL-lactide/glycolide copolymer) was prepared using a solvent formulation of dimethyl carbonate (DMC), formic acid and deionized (DI) water with the following ratio, 99:0.5:0.5 (v/v), respectively. Due to its low conductivity, DMC was not electrosprayed in the cone-jet mode. To enable its stability in this spray regime, traces of formic acid and DI water were added to the bulk DMC formulation. Fresh solutions were magnetically stirred continuously for 120 min at room temperature, vortexed and sonicated in an ultrasonic bath for 30 min to minimize the formation of microbubbles prior to electrospraying. Solutions were fed using a programmable syringe pump (Harvard Apparatus Pump 11 Plus) connected to the ES apparatus using (Pumpsil) Pt-cured silicon tubing. The solution was electrosprayed in the cone-jet mode at 1 mL h^{-1} using a dual-electrode configuration (i.e. needle and extractor plate) with one 19G ($Ø_{OD}$ = 1070 μm, $Ø_{ID}$ = 690 μm) stainless steel ES emitter (vertically) positioned concentrically 1 mm above a 4 mm diameter extractor hole opening. Care was taken to avoid misalignment between the nozzle and the extractor hole, which may cause the jet to discharge asymmetrically leading to an electrical short between the two components. The region between the emitter and extractor plate is known as the 'jet-forming region' and the distance between the extractor and LN_2 collector is known as the 'spray region'. The spray region was kept constant at 40 mm, an optimized distance to keep the field strength sufficiently high yet prevent droplet freezing at the capillary exit ensuring the nozzle temperature remained above the Leidenfrost temperature. Additionally, this particle transport distance held above the nitrogen vapor layer limited air viscous drag, spray drift and space charge effects.

The electrodes were maintained at different potentials to achieve the desired electric field with $V_{NEEDLE} > V_{EXTRACTOR} > V_{COLLECTOR\ (GND)}$. The voltages applied (using a Glassman High Voltage Power Supply, Glassman Europe Ltd, UK) to the needle and extractor were 10.2 kV and 7.0 kV, respectively, producing electric field strengths of 102.0 kV cm^{-1} (between emitter and extractor) and 1.75 kV cm^{-1} (between extractor and LN_2 free

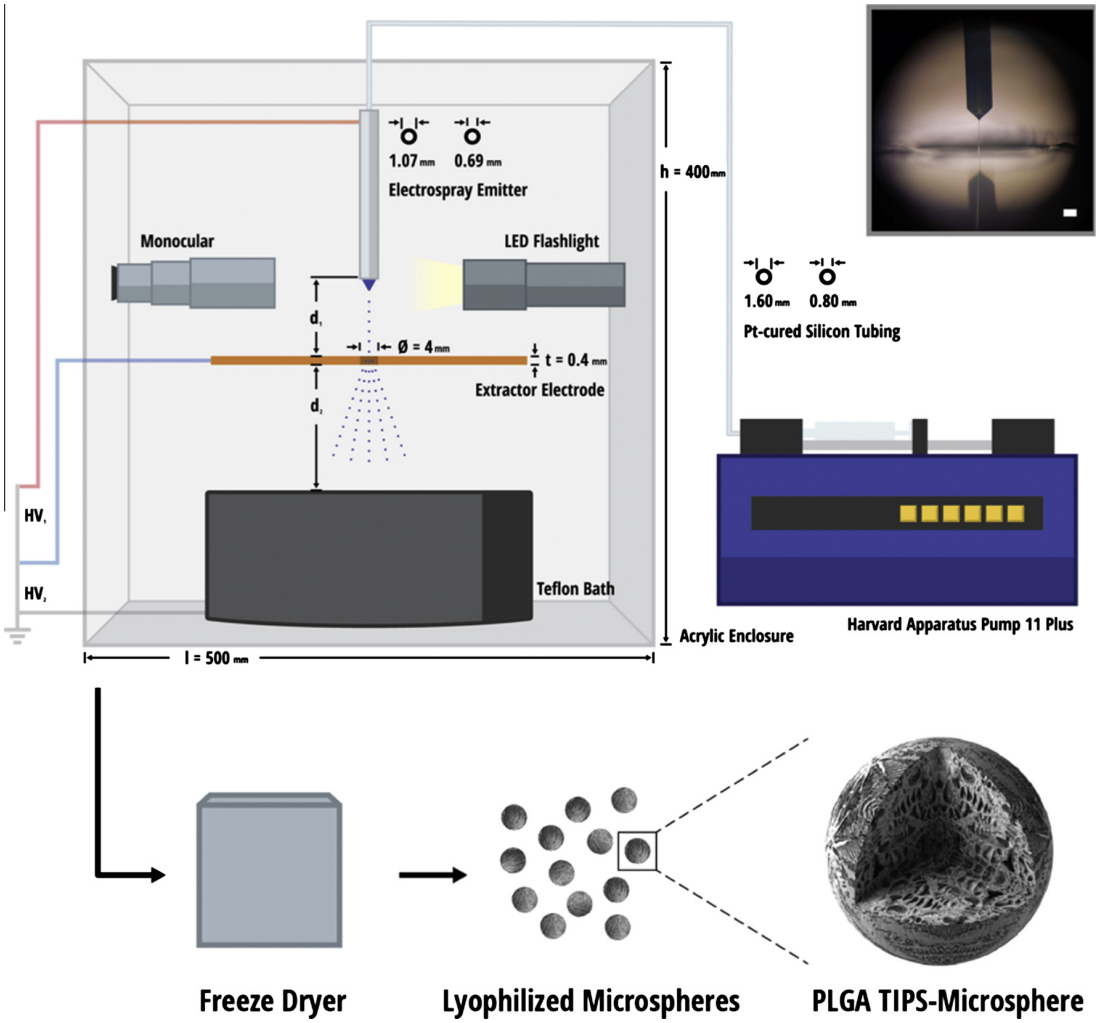

Fig. 1. Schematic representation of the experimental ES configuration confined within a 8 mm thick Perspex enclosure used for this study. Distances, d_1 and d_2 were constantly held at 1 mm and 40 mm, respectively, for optimized collection into the Teflon cryogenic vessel. Distances remained constant throughout the investigation. Lyophilisation of collected PLGA TIPS microspheres is also shown after the ES-synthesis step. (Top right) Photo of ES in the cone-jet mode. Scale bar: 500 μm.

surface). The electric field driving the droplets between the extractor electrode and the collector was high enough to avoid reversal of the droplet motion near the extractor, maintaining control over the charged droplet speed and trajectory. The back-illuminated spray was monitored visually with a StereoZoom 20× microscope and electrically by measuring current emitted, fly-back (at the extractor electrode) and current collected. Particles were collected in a liquid nitrogen bath (40 mm below the extractor plate) held within a non-stick Teflon casing to rapidly induce the phase separation. ES-emission was performed for 60 min and collected particles were promptly transferred to a freezer (−80 °C) and subsequently lyophilized for 24 h in a freeze dryer (LTE Scientific Ltd, Oldham, UK). Post-lyophilisation, particles were stored in their containers for characterization.

A scaling law was applied prior to solution preparation describing the dependency of the diameter of electrosprayed droplets on the physical properties of the liquid being atomized. Regardless of the scaling law considered, the solution electrical conductivity (K) and flow rate (Q) at which the liquid are fed are the primary parameters that control the overall size of ES particles. Droplet sizes were estimated using:

$$d \approx G(\varepsilon)\left(\frac{Q\varepsilon\varepsilon_0}{K}\right)^{\frac{1}{3}}, \quad (1)$$

where d is the droplet diameter, $G(\varepsilon)$ is an empirical function of the order unity, Q is the solution flow rate, ε is the dielectric constant of the liquid, K is the electrical conductivity of the solution, and ε_0 is the permittivity of free space [36]. If a stable cone-jet is preserved, flow rates can only be varied within a certain range defining the ES stability regime. In this case, electrical conductivity was sufficiently raised by adding trace amounts of formic acid and DI water to subsequently decrease droplet diameters. Liquid flow rates were adjusted to 1 mL h^{-1}, 2 mL h^{-1}, 5 mL h^{-1}, 10 mL h^{-1}, 20 mL h^{-1} and 30 mL h^{-1} to manufacture particles of six different sizes.

2.3. Solution conductivity measurements

The electrical conductivity was inferred by measuring the electric current passing through a column of liquid of known length and cross-sectional area connecting two opposite electrodes. Current–Voltage (I–V) measurements were performed at room temperature using a Keithley 4200-SCS (Semiconductor Characterization System) probe station and the mean resistance (R) was read out. Solution conductivities were subsequently calculated using the following formulas:

$$\rho = \frac{RA}{L}, \quad (2)$$

and,

$$\sigma = \frac{1}{\rho}, \quad (3)$$

where ρ (Ω m) is the resistivity, R (Ω) is the resistance, A (m^2) is the cross-sectional area of the column, L (m) is the length between both electrode tips and σ (S m^{-1}) is the solution conductivity. Conductivities were used to estimate droplet diameters using Eq. (1) for particles synthesized at 1 mL h^{-1} as demonstration of the smallest TIPS microsphere that could be manufactured within the ES stability regime.

2.4. Scanning Electron Microscopy (SEM)

TIPS microsphere populations were structurally characterized via SEM to examine their exterior morphologies. Samples were mounted onto aluminum stubs via adhesive carbon tabs and sputter-coated (Quorum Technologies, Q150R) with a thin layer of gold (Au) (typically a few nm) for 180 s in an argon atmosphere. Particles were imaged under a scanning electron microscope (JEOL JSM-7401F) equipped with a Gatan digital camera at an accelerating voltage of 1.0 kV and working distance of 5 mm. Micrographs were captured at several magnifications.

2.5. Focused Ion Beam (FIB)

Internal morphologies of small (~10–20 μm) and large (~200–250 μm) TIPS microspheres were analyzed by SEM after cutting with an FIB (Carl Zeiss XB1540 CrossBeam FIB). Particles were loaded onto specimen holders and prepared using the same techniques as described for SEM analysis. In situ three-dimensional cuts of rectangular cross-section were performed over deposits of particles using a finely focused beam of gallium (Ga^+) ions. Low beam currents selected for milling were typically in the range of 500 pA to 1 nA between subsequent shots of milling process to ensure minimal damage to the polymer matrix. After the initial milling, polishing was carried out at a lower beam current (typically 100 pA) in order to minimize the surface roughness induced by the initial higher current milling. Particle cross-sections were captured after milling using gallium-free imaging by a thermal field emission scanning electron microscope (FE-SEM), integrated into the FIB system.

2.6. Morphologi G3SE

Particle size and shape analysis were evaluated using the Morphologi® G3SE system (Malvern Instruments, Malvern, UK); a microscopic image analysis-based particle characterization system. Samples prepared at two different flow rates, 1 mL h^{-1} and 15 mL h^{-1} were loaded into an aluminum sample entrainment spool (SES) (sprayed with anti-static spray), dry-dispersed using the instruments sample dispersion unit (SDU) and then prepared according to a standard operating procedure (SOP). A gas injection pressure of 1 bar (at 0.05 bar increments) was applied to the SES to cause turbulent flow within the chamber and even mixing of the particles. 19 mm^3 of sample was dispersed (homogenously distributed without particle–particle collision) with a sample settling time of 180 s and imaged through a 20×-magnification objective (Nikon CFI 60 brightfield/darkfield). Five scan areas were distributed across the dispersion area and the results combined comparing both small (prepared at 1 mL h^{-1}) and larger (prepared at 15 mL h^{-1}) ES TIPS microspheres. Two key particle size and shape factors were reported: (i) Circular Equivalent Diameter (CED); the diameter of a circle with the same area as the projected area of the particle image and, (ii) High Sensitivity Circularity (HSC); a measure of the closeness of a particle shape to that of a perfect circle: a value of 1 represents a perfect circle and an irregular shape will have a value less than 1.

2.7. Confocal Raman microscopy

Prior to analysis, samples were mounted on stainless steel specimen stubs (Agar Scientific, UK). Raman spectra acquisition and mapping images were obtained using a WiTec Alpha 300R (LOT Oriel, UK) operating a 0.3 W single frequency 785 nm solid state diode laser (Toptica, USA), a 20× objective lens and an Acton SP2300 triple grating monochromator/spectrograph (Princeton Instruments, USA). Spectra were recorded over the wavenumber range 0–3200 cm^{-1} at a mean resolution of 3 cm^{-1}. Images were created by mapping the intensity of the peak with center wavenumber 1763 cm^{-1} over a 175 × 175 pixel grid, covering an area of 175 μm × 175 μm. Images were also recorded in vertical stacks of horizontal slices, at 12.5 μm height intervals.

2.8. Mercury intrusion porosimetry

To determine the porosity/void fraction of small (~10–20 μm), medium (~100–150 μm) and large (~200–250 μm) particles, microsphere samples were each weighed and added to a glass penetrometer suitable for powder samples. The penetrometer was sealed and the sample analyzed using an AutoPore IV 9500 mercury (Hg) porosimeter (Micromeritics, UK) at pressures in the range 3 kPa to 207 MPa. Hg intrusion into the sample was analyzed using the Washburn equation in order to determine the pore diameter distribution and data was recorded on in-built AutoPore software;

$$D = -\frac{4\gamma}{P}\cos\theta, \tag{4}$$

where D is pore diameter, γ is the surface tension of Hg at 20 °C, which is assumed to be 0.485 N m^{-1}, P is the applied pressure, and θ is the contact angle between the Hg and the porous solid, which is assumed to be 130° [37].

2.9. Thermogravimetry (TG)

Thermogravimetric analysis (TGA) was performed on ES-PLGA TIPS microspheres and PLGA granules (as-received) from Corbion Purac (Netherlands) using a NETZSCH STA 449C TGA system. The instrument's thermobalance and ceramic crucible were calibrated prior to measurement in a vacuum-tight furnace chamber. Data were recorded from 25 to 45 °C with a constant heating rate of 1 °C min^{-1} in a nitrogen atmosphere at 0.5 bar. Measurements were averaged for triplicate readings and the mean thermograms displayed.

2.10. Synthesis of dye-loaded PLGA TIPS microspheres

R6G-loaded PLGA microspheres were synthesized following the same method reported earlier (with non-dye-loaded PLGA microspheres). Briefly, a single mixture of 5% (w/v) polymer solution of PLGA (using the original solvent formulation) loaded with R6G dye at 10 ppm was prepared. The dye was dissolved following continuous stirring for 120 min at room temperature and 30 min sonication to form a dye-PLGA blend. Using the same ES-configuration as seen in Fig. 1, the solution was electrosprayed in the cone-jet mode at 1 mL h^{-1}, 15 mL h^{-1} and 30 mL h^{-1} each for 30 min into a glass beaker (externally wrapped in aluminum foil) containing LN_2 surrounded by a cryogenic vessel also topped with LN_2. The vessel minimized LN_2 evaporation and balanced the heat capacity between beaker and vessel; both were electrically grounded components. A voltage drop ranging from 2.8 to 3.4 kV between the emitter and extractor (charged at 8.0 kV) generated sufficiently high electric fields to produce a stable cone-jet mode for the three flow rates. A second field between extractor electrode and LN_2 free surface held at 2.0 kV cm^{-1} facilitated the acceleration and trajectory of particles into the cryogenic medium held on an equipotential surface. Particles were collected for 30 min and promptly transferred to a freezer (−80 °C) and subsequently lyophilized for 24 h in a freeze dryer.

NB: Only a small concentration of active agent was purposefully chosen to avoid significant changes to the conductivity of the PLGA solution. The choice of active agent loading is not a limitation of the ES-based synthesis protocol.

2.11. Encapsulation Efficiency (EE)

Freeze-dried R6G-loaded PLGA TIPS microspheres for small (~10–20 μm), medium (~100–150 μm) and large (~200–250 μm) particles with known dye loading concentrations (10 ppm) and masses were immersed and re-dissolved back into the ES solvent formulation of DMC, formic acid and DI water with the following ratio, 99:0.5:0.5 (v/v) to each produce a 1% (w/v) concentration solution for each sample. All three samples were first agitated and magnetically stirred continuously for 360 min at ambient temperature under sealed conditions to release the total content of R6G dye entrapped within the polymer matrix. Following centrifugation, supernatants were collected, filtered (Millipore, pore size 0.45 μm) and the total R6G content determined by UV–Visible Spectroscopy (Shimadzu UV-1800 Spectrophotometer). Absorption spectra were recorded over the spectral range 300–800 nm (1 nm resolution) using quartz cells with a 10 mm path length. R6G peaks were detected at 515 nm for each sample. The encapsulation efficiencies (EE) were calculated according to the following equation:

$$EE\ (\%) = \frac{Total\ amount\ of\ dyein\ PLGA\ microspheres}{Total\ amount\ of\ dye\ loading} \times 100, \tag{5}$$

where the total amount of dye in the microspheres is the amount of dye encapsulated in/on the polymer and the theoretical dye content is the amount of dye added to the polymer solution for ES-synthesis. The dye contents were then calculated by reference to a standard calibration curve, formed from 6 different concentrations (0.5–150 ppm) in the same solvent. The calibration curve was found to be highly linear and reproducible, with a coefficient of determination (R^2) of $\geqslant$0.98. All measurements were performed in triplicate and averaged.

2.12. Dissolution testing

Dissolution studies were performed by dispersing dry TIPS microspheres (at known quantities) in distilled water. R6G-loaded PLGA particulates were prepared at 1% (w/v) concentrations for each release sample and magnetically stirred at 37 °C for 7 days. At predefined time intervals, aliquots of 2 mL of the dissolution medium were withdrawn, centrifuged and filtered (Millipore, pore size 0.45 μm). After spectroscopic measurement, the same volume of dissolution medium withdrawn was returned to the same sample flask (i.e. not replaced with fresh medium). Detection of the released dye was measured by analyzing the fluorescence emission at 515 nm peaks and the amount of R6G released was determined by interpolation from a standard calibration curve. *In vitro* release spectra were recorded in triplicate and data shown is the mean of the results. Error bars are indicated on cumulative release curves and relative standard deviation (RSD) for the three measurements remained consistently $\leqslant$5%.

3. Results and discussion

3.1. Microsphere synthesis

Electrospray synthesis of polymeric microspheres was realized using the experimental setup sketched in Fig. 1. A scaling relation (Eq. (1)) was used to select the parameters required to manufacture particles down to approximately 10 ± 5 μm in diameter. Flow rates and liquid conductivities were varied to prepare TIPS microspheres of different size. The addition of formic acid was used to enhance the electrical conductivity of the ES liquid. Calculated diameters with increasing solution conductivity (by addition of formic acid and DI water between 1 and 6 vol.%) are plotted in Fig. 2 and reveal that particle diameters $\leqslant$5 μm are possible at flow rates of 1 mL h^{-1}.

Fig. 2 demonstrates a monotonically increasing trend for diameter against flow rate for PLGA microspheres prepared between 1 and 30 mL h^{-1}. This also demonstrates that a stable operation of the cone-jet mode was preserved (specifically between 1 and

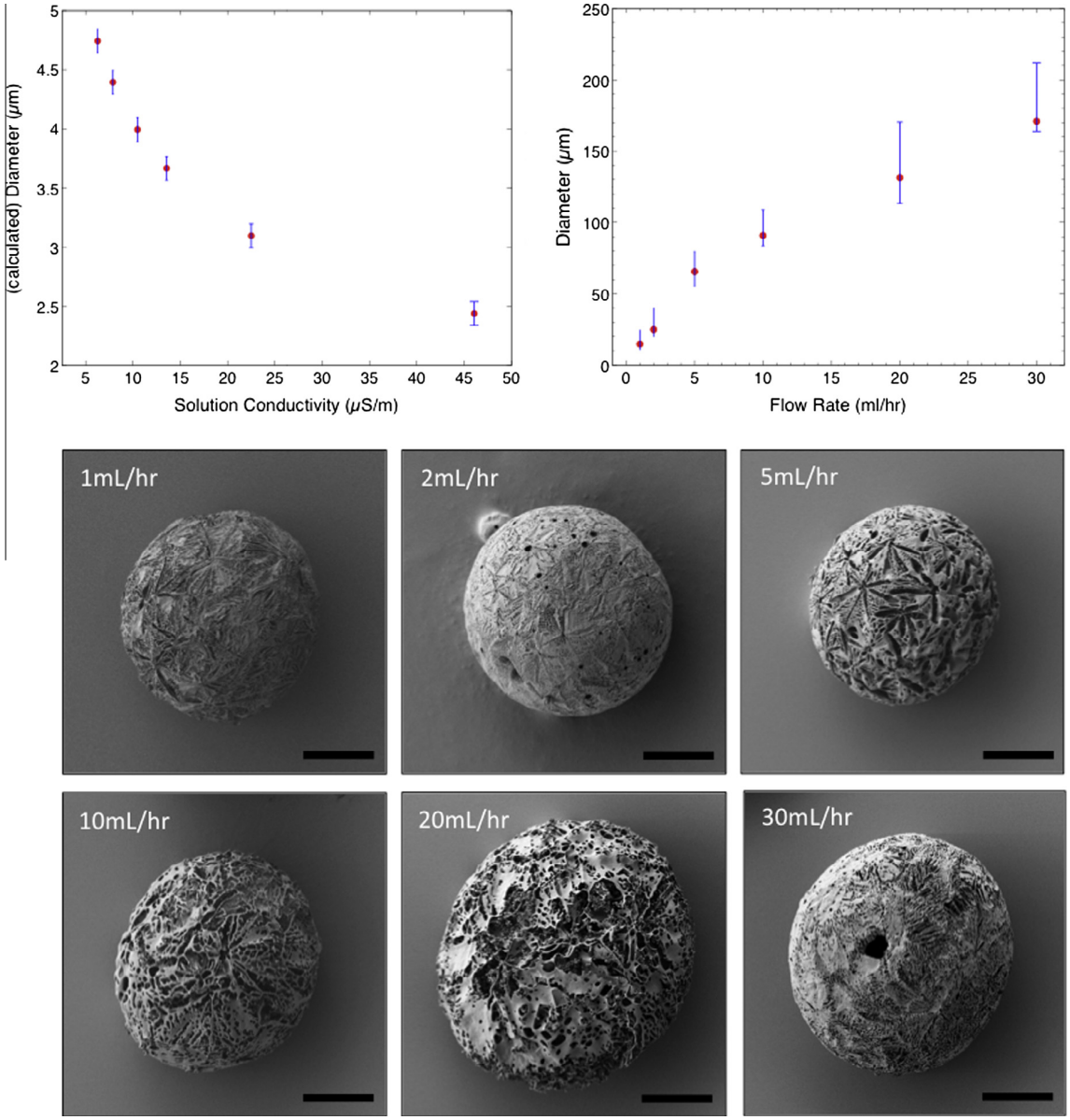

Fig. 2. (Top left) Dependence of the diameter of electrosprayed droplets on solution conductivity (calculated using Eq. (1)). (Top right) Diameter of PLGA TIPS microspheres as a function of flow rate. SEM images revealing representative particle morphology at flow rates: 1 mL h^{-1} (scale bar: 5 μm), 2 mL h^{-1} (scale bar: 10 μm), 5 mL h^{-1} (scale bar: 20 μm), 10 mL h^{-1} (scale bar: 30 μm), 20 mL h^{-1} (scale bar: 40 μm), 30 mL h^{-1} (scale bar: 50 μm).

15 mL h^{-1}), as the flow rate can only be varied within a certain range within the ES stability domain. The addition of small amounts of dopants (i.e. formic acid and DI water) to the solvent enabled particles to be sprayed across a range of flow rates while preserving other physical properties, such as the bulk solvent of DMC (99%). Ensuring the bulk preservation of DMC in the solvent was critical to synthesizing particles as prepared previously [33]. It must also be noted that Fig. 2 (graph, right) demonstrates the standard deviations in diameter for microspheres electrosprayed at larger flow rates (i.e. 20 mL h^{-1} and 30 mL h^{-1}) were greater than those sprayed at low flow rates. Overall, we have demonstrated that approximate control over the size of the novel TIPS microspheres can be provided by alterations in solution conductivity and liquid flow rate, as the droplet diameter increases monotonically with both parameters. Fig. 2 shows the respective SEM images for ES PLGA TIPS microspheres prepared at the six flow rates.

3.2. Particle size and shape analysis

To assess particle shape preservation, size and shape analysis was evaluated on two different microsphere samples prepared using flow rates of 1 mL h^{-1} and 15 mL h^{-1} using an extensive screening process to yield quantifiable size and shape information for thousands of particles. Shape and size affect the bulk behavior of particles (in powders) and, more importantly, can determine biomedical application. In this case, the two flow rates chosen demonstrate control of the electrospray technique to manufacture TIPS microspheres of different sizes by simple variation of one processing parameter, and additionally represent the variation in particle properties when prepared using ES atomization. Both samples were successfully dispersed with the sample dispersion unit and data were interpreted using the in-built Morphologi software.

Fig. 3a shows the number distributions of Circular Equivalent Diameter (CED). Both samples contain a monodisperse population

of discrete particles with no overlapping, and complete isolation from neighboring particles. There is an absence of fine particles and grains, as a distinct peak is visible for both smaller and larger particles. The smaller particles have a CED mean of 16.77 μm, while that of larger particles is 122.91 μm. Particles prepared at 15 mL h^{-1} also show less polydispersity in terms of size distribution. Polydispersity of particle size may introduce variability in the release rates and the shape of the microsphere can also affect particle interaction with macrophages [6].

Fig. 3b shows the High Sensitivity Circularity (HSC) distributions for the two samples screened, indicating that PLGA samples prepared at 15 mL h^{-1} are fractionally more circular than those prepared at 1 mL h^{-1}. As summarized in Table 1, there was a larger sample size screened at 1 mL h^{-1} due to the smaller particle size and the ability of the instrument to disperse particles equidistantly without neighboring contact. Due to the larger (mean) size of particles prepared at 15 mL h^{-1}, the number of particles screened was fewer to avoid overlapping of microspheres.

3.3. Confocal Raman microscopy

The intensity of the Raman peak with center wavenumber 1763 cm^{-1} was mapped at different depths for both electrosprayed PLGA particles and PLGA granules; the peak corresponds to a stretch of the carbonyl moiety. In order to identify changes in chemical composition across particle types, images were obtained by mapping the peak intensity as a function of XY position. Raman spectra were collected with a five-image z-stack of horizontal images, the focal position being adjusted using a piezo scanner. Each image slice through the particle remained consistently 12.5 μm below the other and demonstrated that PLGA exhibits little variation in structure as a function of position in either structural form (see Supporting Information, Fig. S1). The one significant variation, around 440 cm^{-1}, came from the silicon substrate on which particles were mounted. Lighter regions of the image signify regions of high peak intensity in that section of the particle; darker regions signify lower peak intensity. Overall, spectra revealed that as anticipated, electrosprayed PLGA microspheres demonstrated the same spectra as PLGA prior to electrospray processing. The results also reveal that the solvent formulation used in electrospraying has not affected the composition of the material, and verify the complete sublimation of solvent from the particles post-lyophilisation.

Table 1
Summary of size and shape characteristics for particles prepared at 1 mL h^{-1} and 15 mL h^{-1}.

Property	ES PLGA (at 1 mL h^{-1})	ES PLGA (at 15 mL h^{-1})
Particles screened	11,349	6267
CED (μm) mean	16.77	122.91
HSC mean	0.774	0.787

3.4. Mercury intrusion porosimetry

Porosity of spherical compacts was investigated for three particle sizes. Results revealed a clear dependence of particle size on void fraction within particles, as seen in Table 2. Data were verified by SEM image analysis that provided information from three-dimensional cuts of the porous structure using a Focused Ion Beam (FIB). Fig. 4 illustrates how porosity decreases with increasing particle size. This finding suggests that smaller particles would have a shorter release profile than larger particles, as water can penetrate and intrude the pores more easily.

Each composition exhibited a smooth surface skin, peppered with pores often arranged in a chevron-like pattern, typical of TIPS microspheres, along with a large internal cavity [33]. FIB images exposed interconnected porosity with open channels, ideal for effective transport of release medium, both on the surface of spheres and internally. Unlike characteristic TIPS microspheres synthesized from PLGA (dissolved in only DMC), the internal structure did not contain the channel-like radial tubular macropores reported previously [33,34]. In this case, image analysis exposed a snowball-like structure with a continuous distribution of voids within the microspheres and highly anisotropic morphology. During TIPS, the solution is separated into a polymer-rich phase and a polymer-lean phase due to crystallization of the solvent when the temperature of the polymer solution is lower than the freezing point of the solvent. The polymer is expelled from the crystallization front to form a continuous polymer-rich phase. The solvent sublimes to leave pores. This is characteristic of a TIPS particle. The snowball-like structure observed is likely to have resulted from a slightly adjusted solvent formulation for optimal cone-jet ES and/or a different polymer concentration similar to that previously described for emulsion TIPS microspheres [33].

It should, however, be noted that porosimetry results represent only one method of porosity measurements and are strictly limited

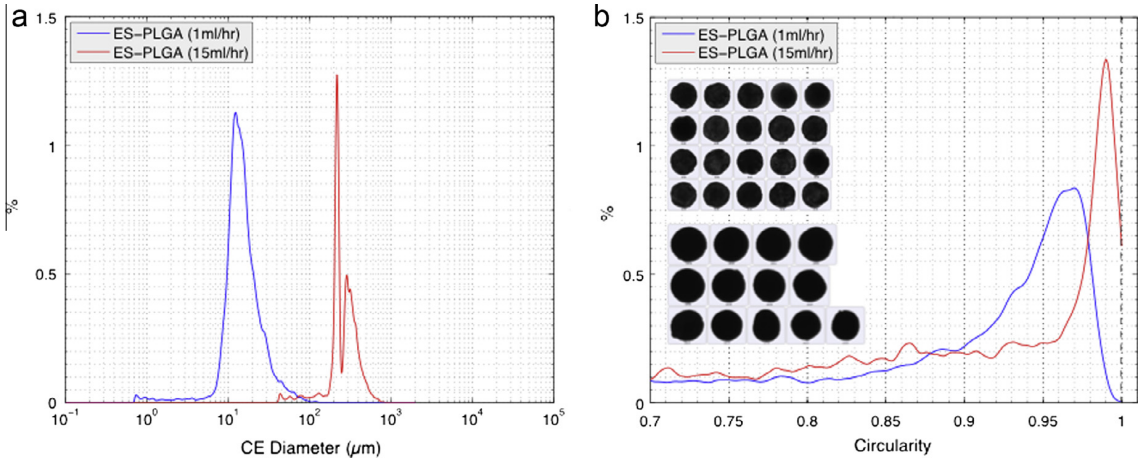

Fig. 3. Distribution plots for (a) CED and (b) HSC for TIPS microspheres. Particles synthesized at 1 mL h^{-1} are indicated with blue lines and particles synthesized at 15 mL h^{-1} are shown in red. Inset in (b) shows the particle images for CED mean of 16.77 μm and HSC mean 0.774 synthesized at 1 mL h^{-1} (top) and particle images for CED mean of 122.91 μm and HSC mean 0.787 synthesized at 15 mL h^{-1} (bottom). (For interpretation of the references to color in this figure legend, the reader is referred to the web version of this article.)

Table 2
Porosimetry measurements for three microspheres of differing sizes.

Property	Small	Medium	Large
Total intrusion volume (mL g^{-1})	14.304	2.783	7.461
Total pore area (m^2 g^{-1})	64.786	0.05	0.135
Apparent (skeletal) density (g mL^{-1})	1.1746	0.2569	0.0843
Porosity (%)	94.38	51.68	38.62

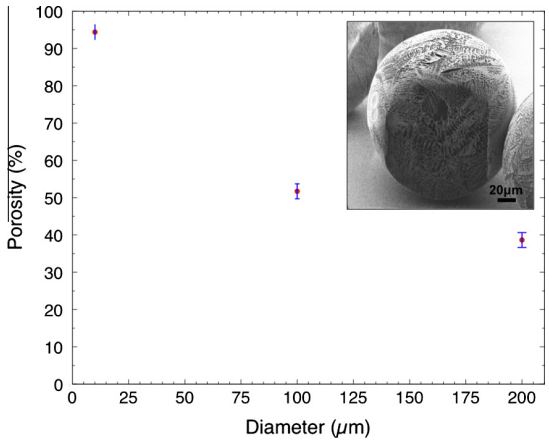

Fig. 4. Size-dependent porosity of PLGA TIPS microspheres. (Inset) FIB three-dimensional cut of a large particle exposing its internal pore network.

to the Washburn equation, which is based on the cylindrical pore assumption and may not hold for all microspheres. The Total Intrusion Volume (TIV) is measured directly during the intrusion process. All other quantities are calculated using the TIV and the Washburn equation. Further control over porosity could be enabled by varying the polymer concentration, polymer composition and solvent formulation.

3.5. Thermogravimetry (TG)

Measurements of mass changes (Δm) due to evaporation, decomposition and interaction with the atmosphere were monitored against controlled and programmed temperature in an inert atmosphere. In order to observe the best comparison, the heating rate and sample mass were kept the same, except that in this case, degradation was compared for a mix of both electrosprayed medium (~100–150 μm) and large-sized (~200–250 μm) PLGA TIPS microspheres and PLGA granules (as received in original form). Due to the low throughput of the process, insufficient masses were produced for the small-sized particles to be measured and therefore comparison was made between particles in the size range ~100–250 μm and the granular sample.

Thermogravimetric analysis of the spherical PLGA TIPS microspheres revealed no physical or chemical changes over the narrow temperature range of biological interest (see Supporting Information, Fig. S2).

3.6. Dissolution testing

The rate of Rhodamine 6G (R6G) release from biodegradable polymeric microspheres can be driven by several mechanisms. The SEM images in Fig. S3(a–c) (see Supporting Information) show the particles have a porous structure and release is therefore influenced predominantly by, (i) desorption of surface-bound dye, (ii) diffusion of dye through the polymer matrix and (iii) erosion of the polymer matrix [38]. For PLGA particles, the surface-bound dye experiences an initial rapid release due to the large surface area of the particles. The porous structure of the polymeric particle enables diffusion and penetration of water and therefore facilitates its hydrolytic degradation and subsequent dye release [39].

In vitro comparison of the release profiles of R6G from particles was made. Particles were categorized as (1) small (~10–20 μm), (2) medium (~100–150 μm) and (3) large (~200–250 μm) with dye concentrations of 10 ppm consistently across all three samples and encapsulation efficiencies >89%. Small particles reported the highest encapsulation efficiency of 93% although more importantly there was no real significant difference between samples. The cumulative R6G release profile for the three compositions in Fig. 5 demonstrates a clear time-dependent release of R6G for all three samples. The size of the microspheres affects the duration of dye release (larger particles lead to more prolonged release). Larger particles are more likely to have dye trapped in the particle center and therefore may not release their entire payload. Moreover a longer study would be required to assess whether particles ever release 100% of the encapsulated agent.

Dissolution studies revealed diffusion of the encapsulated agent in two distinct phases in the cumulative release profile: a first phase in which the release is dominated by diffusion and a second phase with a slower release related to the erosion of the polymer matrix. In the first phase, microspheres released most of their payload ($\geqslant$50%) within 24 h and for smaller particles, release occurred more rapidly. This also indicates that the percentage cumulative release of R6G from highly porous microspheres was significantly higher than that of particles with lower porosities (i.e. of larger sizes). Initial burst release was seen in all three samples due to the incorporated dye being close to, or on, the particle surface thus was instantaneously solubilized out of the particles in release medium. The internal pore network and surface pores act as channels to allow rapid penetration of the dissolution medium into the core. Following this, a second phase revealed a sustained release over one week (~10,080 min) for all particle sizes. Despite this, it must be noted the release profiles of all three cases appear similar; the disparity was believed to stem from differences in particle surface area-to-volume ratio. Similarity in trends suggests the microspheres are highly monodisperse as each particle size follows a similar path. A polydisperse sample would introduce undesired variations in release kinetics.

These results suggest that release kinetics of polymeric carriers can be manipulated by alteration of particle size. Moreover, we have demonstrated the feasibility of controlling the R6G release

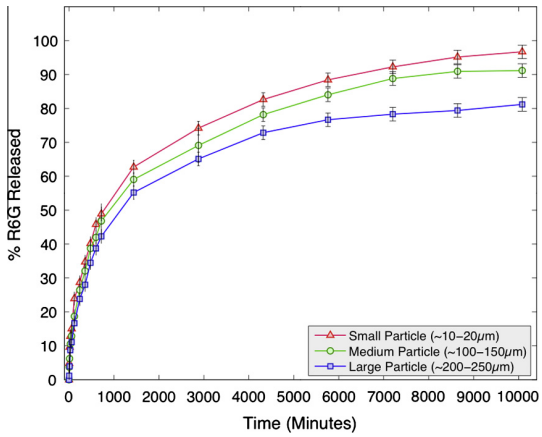

Fig. 5. *In vitro* cumulative R6G release from small (red/triangles), medium (green/circles) and large-sized (blue/squares) PLGA TIPS microspheres. (For interpretation of the references to color in this figure legend, the reader is referred to the web version of this article.)

behavior from porous PLGA TIPS microspheres by careful manipulation of flow rate during synthesis. The microspheres manufactured here have successfully demonstrated long-term delivery (i.e. 1 week) of an active agent, enabling sustained release of the dye without excessive physical degradation (see Supporting Information, Fig. S4). The *in vitro* study reveals a clear dependence of microsphere size on the residual release of the encapsulated dye.

4. Conclusions

We have presented a simple, reproducible and scalable technology offering a complete synthesis protocol for engineering modulated release systems for the next (3rd) generation of release technologies. The promising findings of this study indicate the potential of PLGA TIPS microsphere technologies as vehicles for programmed and controlled release of active agents with the possibility to incorporate bioactive molecules.

We have systematically investigated the effect of size and shape on active ingredient encapsulation and release kinetics. Dye dissolution data revealed evidently that release can be manipulated by carefully controlling and adjusting effective porosities, regulated by particle size. As size decreases, activity rate of the carrier increases. Processing can be adjusted to tailor pore structure (radial or interconnected) and void fraction (i.e. skeletal porosity) as mercury intrusion porosimetry results reveal. More importantly, dye encapsulation does not significantly alter the snowball-like morphology of microspheres. Thermogravimetric measurements reveal no mass degradation across body temperatures and verify the potential for use in *in vivo* clinical investigation. Overcoming and controlling burst release with the microparticle compositions described in the current study remains a challenge, but this will formulate the next stage in the TIPS microsphere development using ES-synthesis techniques.

Advantages of the ES-synthesis route include the ease of use, low cost and parametric control over the size of the polymeric microspheres. It provides a chemical-free, sustainable and scalable solution that has the potential to manufacture particles of controlled sizes and morphology to address a plethora of therapeutic challenges. Although the synthesis process has not yet been refined, further improvement can enable us to extend the protocol to other polymer systems and manufacture bespoke TIPS particles on demand. Follow-on studies are needed to elucidate the findings presented here, including alteration of solvent formulation, composite polymer blends, active agent loading and denaturation effects on polymer matrix with increased loading.

Competing interests

I/We have no competing interests.

Authors' contributions

SM performed the research reported here including experimental design, experimental work, analysis and interpretation of data, statistical analysis and drafted (and revised) the manuscript; WN carried out SEM imaging, FIB milling of the polymer particles and contributed partially to sample preparation in the experimental section; JB performed partial characterization of the particles as well as statistical analysis and contributed partially to sample preparation in the experimental section; JT participated in the design of the study and revised the article critically for important intellectual content; AG partially conceived, designed and coordinated the study as well as contributed to key manuscript revisions for intellectual content; AK coordinated the study, provided critical support for experimental work and revised the article critically for important intellectual content; RD conceived, designed and coordinated the study as well as contributed to key manuscript revisions for intellectual content. All authors gave final approval for publication.

Acknowledgements

The authors gratefully acknowledge: (i) the financial support provided by the Engineering and Physical Sciences Research Council (EPSRC), United Kingdom, through a Doctoral Training Award (ii) The UCL Institute of Biomedical Engineering (IBME) Yale-UCL Medical Technologies Collaborative (MTC) via an EPSRC Global Engagement award (EP/K004506/1) (iii) The financial support provided by the Department of Biomedical Engineering at Yale University. This work was undertaken at UCL/UCLH which receives funding from the Department of Health's NIHR as a comprehensive Biomedical Research Centre. Finally, Mr. S.A. Malik would like to thank Mr. Clemens Tummelsthammer for engaging discussions with the dissolution studies and equally Dr. Panagiotis Sofokleous for technical assistance with freeze drying the samples.

Appendix A. Supplementary material

Supplementary data associated with this article can be found, in the online version, at http://dx.doi.org/10.1016/j.jcis.2016.01.021.

References

[1] K. Park, Controlled drug delivery systems: past forward and future back, J. Control. Release 190 (2014) 3–8, http://dx.doi.org/10.1016/j.jconrel.2014.03.054.
[2] A.K. Sheela, Microspheres Market – Global Industry Analysis, Size, Share, Growth, Trends and Forecast (2013–2019). <www.researchmoz.us> (accessed: 06/2015).
[3] E. Campos, J. Branquinho, A.S. Carreira, A. Carvalho, P. Coimbra, P. Ferreira, M. H. Gil, Designing polymeric microparticles for biomedical and industrial applications, Euro. Polym. J. 49 (2013) 2005–2021, http://dx.doi.org/10.1016/j.eurpolymj.2013.04.033.
[4] A. Jaworek, Micro- and nanoparticle production by electrospraying, Powder Technol. 176 (2007) 18–35, http://dx.doi.org/10.1016/j.powtec.2007.01.035.
[5] S. Mitragotri, P.A. Burke, R. Langer, Overcoming the challenges in administering biopharmaceuticals: formulation and delivery strategies, Nat. Rev. Drug Discov. 13 (2014) 655–672, http://dx.doi.org/10.1038/nrd4363.
[6] J.A. Champion, S. Mitragotri, Role of target geometry in phagocytosis, Proc. Natl. Acad. Sci. U.S.A. 103 (2006) 4930–4934, http://dx.doi.org/10.1073/pnas.0600997103.
[7] S.M. Moghimi, A.C. Hunter, J.C. Murray, Long-circulating and target-specific nanoparticles: theory to practice, Pharmacol. Rev. 53 (2001) 283–318.
[8] M. Okubo, Y. Konishi, H. Minami, Production of hollow polymer particles by suspension polymerization, Colloid Polym. Sci. 276 (1998) 638–642, http://dx.doi.org/10.1007/s003960050291.
[9] R. Arshady, Microspheres and microcapsules: a survey of manufacturing techniques. Part 1: Suspension cross-linking, Polym. Sci. Eng. 29 (1989) 1746–1758, http://dx.doi.org/10.1002/pen.760292404.
[10] Y. Zhang, Y. Guan, S. Yang, J. Xu, C.C. Han, Fabrication of hollow capsules based on hydrogen bonding, Adv. Mater. 15 (2003) 832–835, http://dx.doi.org/10.1002/adma.200304315.
[11] M. Fujiwara, K. Shiokawa, T. Kubota, Direct encapsulation of proteins into calcium silicate microparticles by water/oil/water interfacial reaction method and their responsive release behaviors, Mater. Sci. Eng. C 32 (2012) 2484–2490, http://dx.doi.org/10.1016/j.msec.2012.07.030.
[12] Lyophilisation – Europe. <www.smi-online.co.uk/pharmaceuticals/uk/lyophilisation-freeze-drying-pharma-andbiopharma> (accessed: 06/2015).
[13] H. Ghanbar, C.J. Luo, P. Bakhshi, R. Day, M. Edirisinghe, Preparation of porous microsphere-scaffolds by electrohydrodynamic forming and thermally induced phase separation, Mater. Sci. Eng. C 33 (2013) 2488–2498, http://dx.doi.org/10.1016/j.msec.2012.12.098.
[14] B. Almería, W. Deng, T.M. Fahmy, A. Gomez, Controlling the morphology of electrospray-generated PLGA microparticles for drug delivery, J. Colloid Interface Sci. 343 (2010) 125–133, http://dx.doi.org/10.1016/j.jcis.2009.10.002.
[15] B. Almería, T.M. Fahmy, A. Gomez, A multiplexed electrospray process for single-step synthesis of stabilized polymer particles for drug delivery, J. Control. Release 154 (2011) 203–210, http://dx.doi.org/10.1016/j.jconrel.2011.05.018.
[16] A. Bohr, M. Yang, S. Baldursdóttir, J. Kristensen, M. Dyas, E. Stride, M. Edirisinghe, Particle formation and characteristics of celecoxib-loaded poly

(lactic-co-glycolic acid) microparticles prepared in different solvents using electrospraying, Polymer 53 (2012) 3220–3229, http://dx.doi.org/10.1016/j.polymer.2012.05.002.
[17] A. Bohr, J. Kristensen, E. Stride, M. Dyas, M. Edirisinghe, Preparation of microspheres containing low solubility drug compound by electrohydrodynamic spraying, Int. J. Pharm. 412 (2011) 59–67, http://dx.doi.org/10.1016/j.ijpharm.2011.04.005.
[18] Y. Gao, D. Zhao, M. Chang, Z. Ahmad, X. Li, H. Suo, J. Li, Morphology control of electrosprayed core–shell particles via collection media variation, Mater. Lett. 146 (2015) 59–64, http://dx.doi.org/10.1016/j.matlet.2015.02.013.
[19] L. Nie, G. Zhang, R. Hou, H. Xu, Y. Li, J. Fu, Controllable promotion of chondrocyte adhesion and growth on PVA hydrogels by controlled release of TGF-β1 from porous PLGA microspheres, Colloids Surf., B 125 (2015) 51–57, http://dx.doi.org/10.1016/j.colsurfb.2014.11.010.
[20] P. Suvannasara, K. Siralertmukul, N. Muangsin, Electrosprayed 4-carboxybenzenesulfonamide-chitosan microspheres for acetazolamide delivery, Int. J. Biol. Macromol. 64 (2014) 240–246, http://dx.doi.org/10.1016/j.ijbiomac.2013.12.012.
[21] G. Zhang, R. Hou, D. Zhan, Y. Cong, Y. Cheng, J. Fu, Fabrication of hollow porous PLGA microspheres for controlled protein release and promotion of cell compatibility, Chin. Chem. Lett. 24 (2013) 710–714, http://dx.doi.org/10.1016/j.cclet.2013.05.011.
[22] S.D. Nath, S. Son, A. Sadiasa, Y.K. Min, B.T. Lee, Preparation and characterization of PLGA microspheres by the electrospraying method for delivering simvastatin for bone regeneration, Int. J. Pharm. 443 (2013) 87–94, http://dx.doi.org/10.1016/j.ijpharm.2012.12.037.
[23] A.G. Bailey, Electrostatic Spraying of Liquids, J. Wiley & Sons, NY, USA, 1988.
[24] L.F.R.S. Rayleigh, On the equilibrium of liquid conducting masses charged with electricity, Philos. Mag. 14 (1882) 184–186, http://dx.doi.org/10.1080/14786448208628425.
[25] O.V. Salata, Tools of nanotechnology: electrospray, Curr. Nanosci. 1 (2005) 25–33, http://dx.doi.org/10.2174/1573413052953192.
[26] G.F.R.S. Taylor, Disintegration of water drops in an electric field, Proc. R. Soc. London, Ser. A 280 (1964) 383–397.
[27] M. Cloupeau, B. Prunet-Foch, Electrostatic spraying of liquids in cone-jet mode, J. Electrost. 22 (1989) 135–159, http://dx.doi.org/10.1016/0304-3886(89)90081-8.
[28] M. Cloupeau, B. Prunet-Foch, Electrostatic spraying of liquids: main functioning modes, J. Electrost. 25 (1990) 165–184, http://dx.doi.org/10.1016/0304-3886(90)90025-Q.
[29] A. Gomez, K. Tang, Charge and fission of droplets in electrostatic sprays, Phys. Fluids 6 (1994) 404–414, http://dx.doi.org/10.1063/1.868037.
[30] A. Jaworek, Electrospray Technology for Thin-Film Deposition, Nova Science Publishers Inc, NY, USA, 2010.
[31] D. Chen, D.Y.H. Pui, S.L. Kaufmar, Electrospraying of conducting liquids for monodisperse aerosol generation in the 4 nm to 1.8 μm diameter range, J. Aerosol Sci. 26 (1995) 963–977, http://dx.doi.org/10.1016/0021-8502(95)00027-A.
[32] R.I. Mahato, A.S. Narang, Pharmaceutical Dosage Forms and Drug Delivery, CRC Press, USA, 2011.
[33] J.J. Blaker, J.C. Knowles, R.M. Day, Novel fabrication techniques to produce microspheres by thermally induced phase separation for tissue engineering and drug delivery, Acta Biomater. 4 (2008) 264–272, http://dx.doi.org/10.1016/j.actbio.2007.09.011.
[34] H. Keshaw, N. Thapar, A.J. Burns, N. Mordan, J.C. Knowles, A. Forbes, R.M. Day, Microporous collagen spheres produced via thermally induced phase separation for tissue regeneration, Acta Biomater. 6 (2010) 1158–1166, http://dx.doi.org/10.1016/j.actbio.2009.08.044.
[35] R. Ahmadi, N. Mordan, A. Forbes, R.M. Day, Enhanced attachment, growth and migration of smooth muscle cells on microcarriers produced using thermally induced phase separation, Acta Biomater. 7 (2011) 1542–1549, http://dx.doi.org/10.1016/j.actbio.2010.12.022.
[36] J. Fernández de la Mora, The fluid dynamics of taylor cones, Annu. Rev. Fluid Mech. 39 (2007) 217–243, http://dx.doi.org/10.1146/annurev.fluid.39.050905.110159.
[37] E.W. Washburn, Note on a method of determining the distribution of pore sizes in a porous material, Proc. Natl. Acad. Sci. U.S.A. 7 (1921) 115–116.
[38] K.S. Soppimath, T.M. Aminabhavi, A.R. Kulkarni, W.E. Rudzinski, Biodegradable polymeric nanoparticles as drug delivery devices, J. Control. Release 70 (2001) 1–20, http://dx.doi.org/10.1016/S0168-3659(00)00339-4.
[39] G. Schliecker, C. Schmidt, S. Fuchs, R. Wombacher, T. Kissel, Hydrolytic degradation of poly(lactide-co-glycolide) films: effect of oligomers on degradation rate and crystallinity, Int. J. Pharm. 266 (2003) 39–49, http://dx.doi.org/10.1016/S0378-5173(03)00379-X.